# Distributed Power Quality Enhancement Using Residential Power Routers

Shuang Zhao, Zhongjing Wang, Janviere Umuhoza, Alan Mantooth, Yue Zhao, Chris Farnell
Department of Electrical Engineering
University of Arkansas
Fayetteville, AR, 72701, USA
sz009@uark.edu

***Abstract*—To address power quality issues in the residential split-phase distribution systems, a novel residential power router (RPR) is proposed in this paper. It consists of a dual-half bridge (DHB) converter and a split-phase inverter. The DHB provides the galvanic isolation and bidirectional power flow channel for the distributed generation terminal. The split-phase inverter can work as the active power filter, the reactive power compensator, and balance the power of two phases. The power balancing mode is critical to a residential microgrid, especially when the utility grid is not accessible. A proportional quasi-resonance and resonance (PQRR) controller is adopted to eliminate the steady-state error for harmonics compensation. Simulation and experimental results are presented in this paper to validate the feasibility and effectiveness of the proposed RPR for residential applications.**

***Keywords—Compensation; power quality; power router; resonance control;***

## I. INTRODUCTION

In the past decades, a significant amount of research effort has gone into the development of power routing systems for residential energy management applications. The residential power router (RPR) was proposed as a solution of energy management between the on-site distributed energy resources (DER) and the electric grid within a home [1]. Recently, RPR has attracted a lot of attention as a way to monitor and optimize energy usage [2], [3].

In the widely adopted split-phase residential distribution system, the integration of distributed generation (DG) units in grid-connected residential homes introduces many operational challenges that need to be addressed in the design of control and protection systems. Power balancing and power quality issues, including both current harmonics and reactive power compensation, should be carefully addressed to fully harness the potential benefits of the DGs [4].

Meanwhile, nonlinear loads have increased dramatically due to the wide adoption of power electronic systems, such as the power supplies of computers, electric vehicle chargers, and smart home appliances. Power quality problem, especially high harmonics and high reactive power, becomes an obvious issue. It is even more serious in the distribution networks compared with the utility grid[5]-[7]. Centralized active power filters (APF) have been used to improve power quality, but they are not an appropriate method for the residential distribution network, since it is highly distributed [8]. Thus, a distributed APF can be more effective [9].

Another challenge for the RPRs is power balancing. When the utility grid is not available, all the RPRs within one community can be tied together to form a microgrid (MG). In this work, this operating mode is defined as the community mode. Since the community grid is weak compared with utility grid, the power imbalance between the two phases is vital. Extensive research can be found regarding power balancing for three-phase distribution systems [10]-[12]. However, the power imbalance issue for the residential split-phase distribution grid has not been thoroughly addressed yet. The unbalanced load may result in a neutral point voltage shift in the split-phase distribution grid. Thus, compensation of the unbalanced load in a MG is a significant issue that should be addressed.

In this work, the aforementioned power quality issues are addressed by the advanced controls of the RPR. Compared with [13], the power router proposed in this paper can not only manage the DG terminals and mitigate the current harmonics, but also correct the power factor and balance the power between two phases. The tertiary control strategy of the RPR is introduced. The power flow of the fundamental and the harmonics components of the current are analyzed in detail. Based on the power flow analysis, the control strategy for the dual half-bridge (DHB) converter and the split-phase inverter is derived. Both simulations and experiments have been performed to validate the feasibility and effectiveness of the proposed RPR and its control strategy. The results verify that the proposed RPR with the harmonics compensation and power balancing capabilities can effectively improve the power quality of the residential grid.

## II. THE TOPOLOGY AND THE OPEARTION MODE

The circuit topology of the proposed RPR is shown in Fig. 1. It consists of a DHB converter and a split-phase inverter. The battery and residential DERs are connected to the low-voltage (LV) dc bus of the DHB. It provides galvanic isolation for the sensitive dc loads and DERs from the power grid and prevents potential damage of sensitive loads [16].

In this section, the energy management system (EMS) of the RPR is introduced. The EMS of the proposed RPR has

This project is supported by NSF I/UCRC GRid-connected Advanced Power Electronics Systems (*GRAPES*, NSF award number: IIP-1439700)

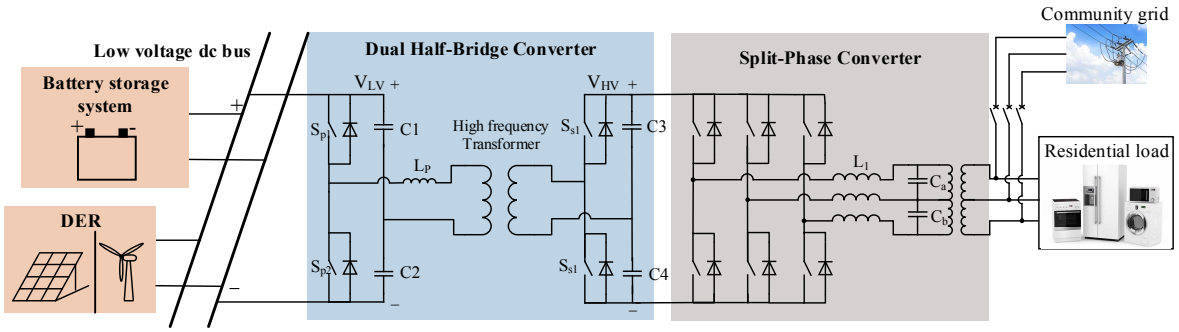


Fig. 1. The topology for the proposed residential power router.

three tertiary control modes, including the grid-connected mode, the community mode and the islanded mode. When the utility grid is accessible, the RPR will operate in the grid-connected mode. The RPR is connected to the utility grid and saves money for the users through daily cycling of battery storage system and DG [14]. When the utility grid is not accessible and the circuit breaker (CB) is open, the RPR will operate in the community mode. All the RPRs in the same community will be inter-tied to form a MG, as illustrated in Fig. 2.

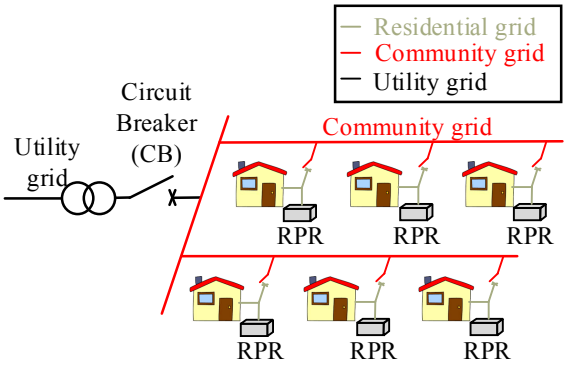


Fig. 2. A typical community connection for the residential

When the community mode is no longer available, each individual RPR disconnects from the community MG and operates as an uninterrupted power supply (UPS) for the load. This is defined as the islanded mode in this work. More details of the tertiary control modes are presented in [14].

For the community mode, the robustness of the system is determined by the total capacity of the RPRs in the system. Compared with grid-connected mode, the community grid is relatively weak. The power quality problems, such as the increased harmonic currents and reactive power, are serious due to the limited capacity [15]. Another issue for the community mode is phase unbalance. It is defined as the condition that loads connected to the two split phases are not equal, which may result in excessive power losses on one phase. For the worst case condition, the voltage on the neutral point could be shifted [15]. Thus, power quality enhancement is necessary.

The traditional RPR only operates to manage the load and DGs at home. For the distributed system, the centralized compensation equipment, such as the unified power factor compensators (UPFC) and APF, are installed to improve the power quality. However, the unsuitable install location may affect the compensation performance [16]. Compared with the centralized approach, distributed compensation using RPRs is more cost effective, since no additional equipment is required, and more robust mitigating a possible single point failure.

## III. THE CONTROL STRATEGY OF DHB

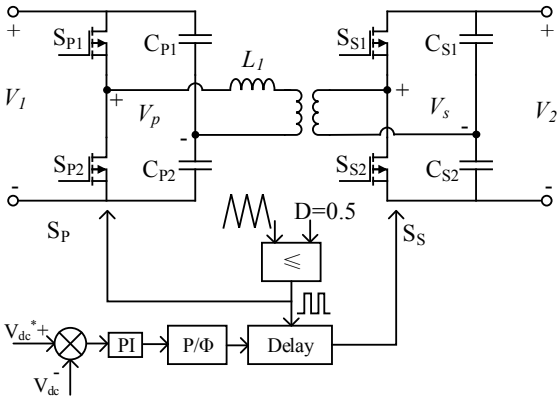


Fig. 3. The control strategy of the DHB converter.

The DHB is controlled to properly balance the power for the inverter and maintain the dc bus voltage. The output power ($P_{out}$) of the DHB can be controlled by the phase-shift angle ($\phi$) [17].

$$P_{out} = \frac{V_1 V_2}{4\pi\omega_s L_1}\phi(\pi - \phi) \quad (1)$$

In grid-connected mode and community mode, the phase-shift angle will be sent to the split-phase inverter to control the output power of the RPR. It should be noted that the power balance between the DHB converter and the split-phase inverter is very important, especially under current control mode of the split-phase inverter. The mismatched power between the DHB and split-phase inverter will result in the overvoltage on the dc bus.

## IV. THE CONTROL STRATEGY OF SPLIT-PHASE INVERTER

In this section, the proposed control strategy of the split-phase inverter will be presented.

### *A. The harmonics compensation*

The harmonics compensation function can be activated when the RPRs are connected to the community grid. As discussed in Section II, in grid-connected mode, the split-phase inverters within a community are tied together to form a community grid. As a kind of weak grid, the power quality is a big issue for the stability of the operation. The main target of grid-connected mode is to send power back to the grid and mitigate power quality problems. In this section, the power flow of the split-phase inverter and grid is analyzed. Based on this analysis, the block diagram of the controller was designed.

The equivalent circuit of the entire system is as shown in Fig. 4. The total current that flows into the split-phase inverter is zero, as shown in (2).

$$I_{Sa} + I_{Sb} = -I_{Sn} \tag{2}$$

where $I_{Sa}$ , $I_{Sb}$ and $I_{Sn}$ are the Phase A, Phase B and neutral bridge output current of a split-phase inverter, respectively. According to (2), the output current can be controlled by two variables, $I_{Sa}$ and $I_{Sb}$. To simplify the control strategy, $I_{Sa} - I_{Sb}$ and $I_{Sa} + I_{Sb}$ are selected to as the control objects. $I_{Sa} - I_{Sb}$ is for the line bridge and $I_{Sa}+I_{Sb}$ is for the neutral bridge. Through the proper adjustment of the reference of $I_{Sa} - I_{Sb}$ and, $I_{Sa}+I_{Sb}$ , the output power of the split-phase inverter can be controlled.

The total apparent power of the split-phase inverter is given by (3). $V_{an}$ and $V_{bn}$ are the Phase A voltage and Phase B voltage of the grid, respectively.

$$S = V_{an} I_{Sa} + V_{bn} I_{Sb} \tag{3}$$

As shown in Fig. 4, all of the current in the circuit can be decomposed into the fundamental component and harmonic components. The relationship of split-phase inverter output current, grid current and load current can be represented by (4), where $I_{Sa\_1}$ and $I_{Sa\_h}$ are the fundamental component and harmonic component of the split-phase inverter Phase A output current, respectively. $I_{Ga\_1}$, $I_{Ga\_h}$, $I_{La\_1}$ and $I_{La\_h}$ are the fundamental component and harmonic component of the Phase A grid output current and Phase A load current, respectively. The relationship of Phase B current is similar.

$$\begin{cases} I_{Sa} = I_{Sa\_1} + I_{Sa\_h} \\ I_{Ga} = I_{Ga\_1} + I_{Ga\_h} \\ I_{La} = I_{La\_1} + I_{La\_h} \end{cases} \tag{4}$$

Because the harmonics compensation mode only considers the harmonics components, the fundamental components are ignored in this case. The current harmonics are desired to be compensated completely by the split-phase inverter. For the ideal condition, the current harmonics are not supposed to flow into the utility grid. The control target equation for harmonic compensation is as shown in (5).

$$I_{Ga\_h} = I_{Gb\_h} = I_{Gn\_h} = 0 \tag{5}$$

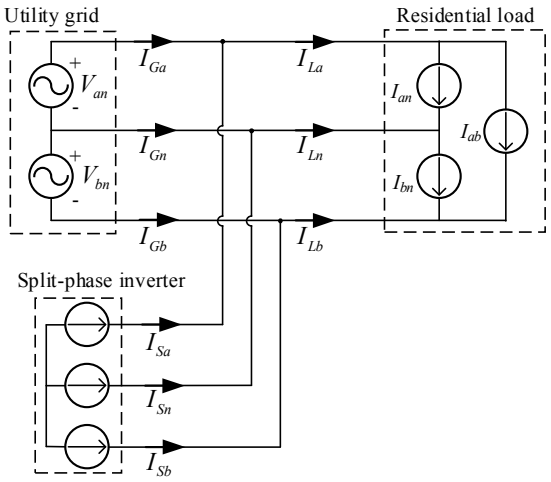


Fig. 4. The power flow analysis of the RPR system.

By substituting (5) into (4), (6) can be derived to obtain the harmonics canceling reference of the inverter.

$$\begin{cases} I_{Sa\_h} - I_{Sb\_h} = I_{La\_h} - I_{Lb\_h} \\ I_{Sn\_h} = -I_{Lb\_h} - I_{La\_h} \end{cases} \tag{6}$$

The harmonic components can be extracted by the Fast Fourier transform (FFT). To reduce the steady-state error of the harmonics, a PQRR controller is used to reduce steady-state error of the current. The expression of the PQRR controller is given by Fig. 5.

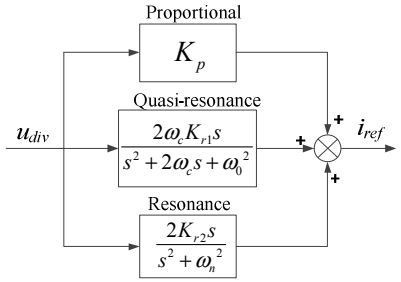


Fig. 5. The block diagram of the PQRR.

A PQRR controller has quasi-resonance, proportional and resonance compensator.

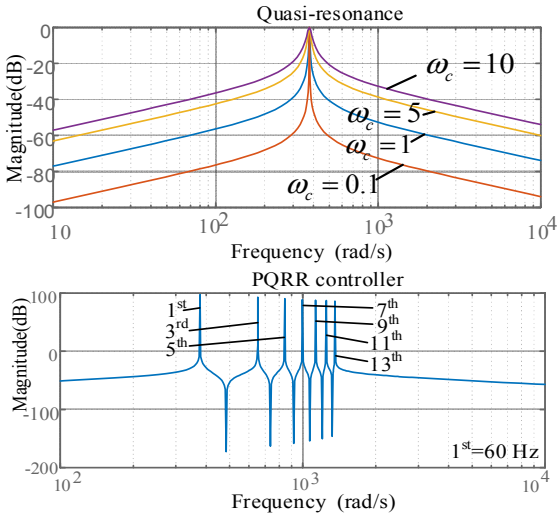


Fig. 6. The Bode plot of the PQRR controller.

The quasi-resonance compensator works to track the fundamental component. Due to its broad bandwidth, it can compensate the fundamental component even when the fundamental frequency shifts.

The higher the $\omega_c$ is, the broader the bandwidth will be. However, the quasi-resonance controller is no longer a non-steady state error compensator. The higher bandwidth will result in lower resonance frequency gain. Therefore, there is a tradeoff when designing the quasi-resonance controller. Since the gain of resonance compensator is infinite at the resonance frequency, it can provide non-steady-state error tracking for the harmonics current. The relationship of gain and resonance frequency is demonstrated in Fig. 6. The pole assignment method can be used for the parameter-based design of the PQRR [19].

### *B. The phase imbalance compensation*

The phase imbalance compensation is designed especially for community mode. The objective of phase imbalance compensation is to move the active power from the heavy-

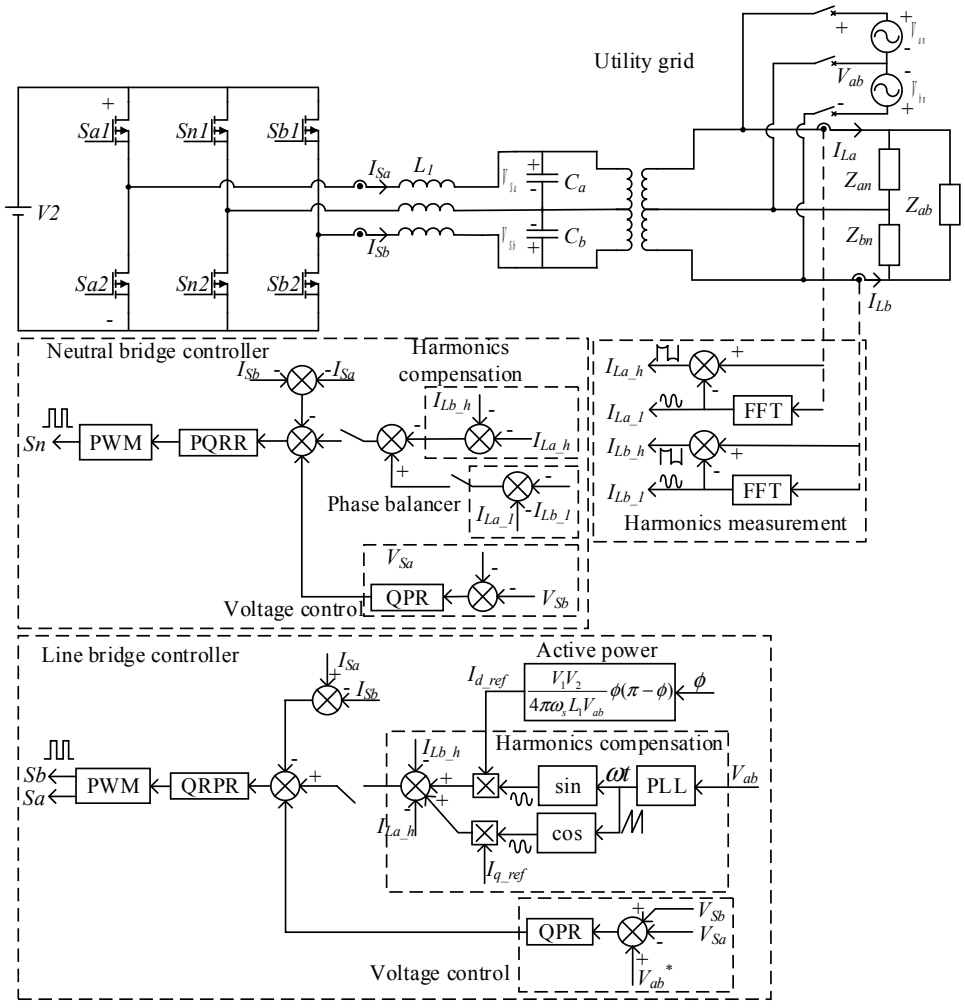


Fig. 7. The control strategy of the split-phase inverter.

loaded phase to the light-loaded phase. Prior to designing the control strategy, the power flow should be analyzed. When the current of two phases is balanced on the utility grid, the control target equation is as shown in (7)

$$I_{Ga\_1} + I_{Gb\_1} = 0 \tag{7}$$

Because the phase balancer only considers the fundamental components, the harmonic components are neglected here. Substitute (7) into (4), the power balancing target equation can be derived as shown in (8).

$$I_{Sn\_1} = -I_{La\_1} - I_{Lb\_1} \tag{8}$$

Based on (8), the power balancer can be realized through controlling the neutral bridge. The power balancing module is shown in Fig. 7.

*C. Islanded mode control strategy*

In Section II, the islanded mode is activated when both the utility grid and community grid are no longer available. To continue supplying reliable electric power to residential appliances through the DG terminals and battery storage system, the split-phase inverter will operate in voltage control mode. The control block diagram is as shown in Fig. 7.

It should be noted that in voltage control mode, the split-phase inverter operates as a slack terminal. The slack terminal is responsible for balancing the power surplus/deficit and stabilizing the bus voltage [20]. Therefore, the under-generation condition will decrease the dc bus voltage whereas the over-generation will increase the dc bus voltage. To prevent the power mismatch condition, the tertiary control should calculate the imbalanced power and send a command to shed the load or limit the generation. A proportional quasi-resonance controller is adopted for the voltage outer-loop of the split-phase inverter. The control block diagram is as shown in Fig. 7.

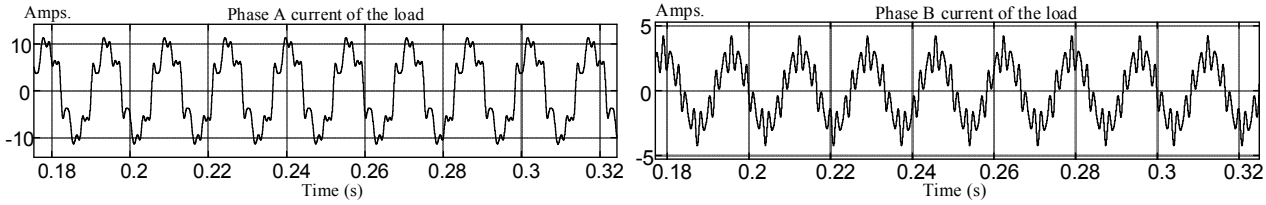


Fig. 8. The load current without compensation.

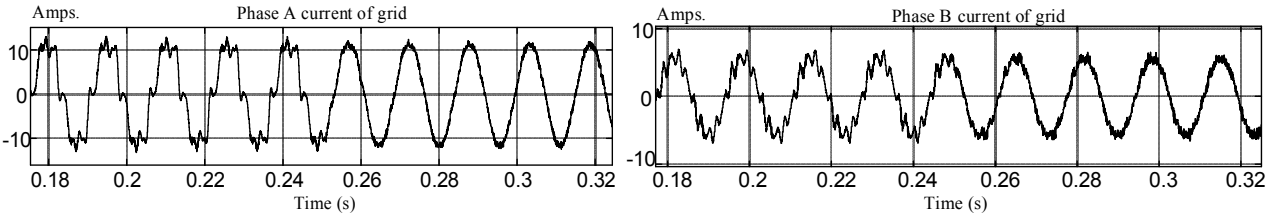


Fig. 9. The load current with harmonics compensation enabled at 0.25 s.

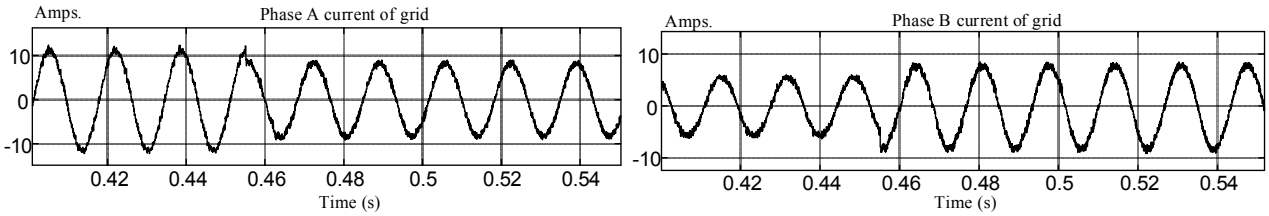


Fig. 10. The load current with phase imbalance compensation enabled at 0.45 s. .

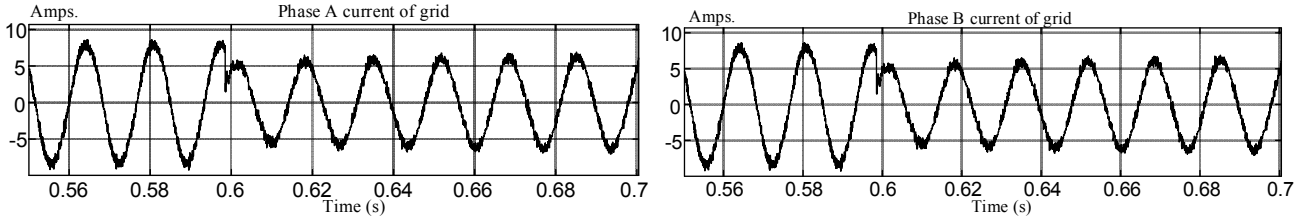


Fig. 11. The load current with reactive power compensation enabled at 0.6 s.

## V. Simulation and Experimental Results

In this section, the functionalities of the proposed RPR are verified through simulation and experiment.

### A. Simulation Studies

The harmonics compensation functions are verified through Simulink® simulation. A MATLAB/Simulink® model is built based on the real parameters of the hardware. It should be noted that the high-frequency harmonic current is relatively low in the residential utility grid. In this paper, the maximum order of the resonance controller is the 13th. In the practical hardware, with a stronger main control unit, the order of the PQRR controller can be higher to guarantee the compensation for high-frequency harmonics.

The ac voltage is 110 V rms for each phase. The input voltage of DHB converter V2 is 400 V and the output voltage of DHB converter V1 is 100 V. The fundamental component of the current is 7 A rms for Phase A and 4 A rms for Phase B.

TABLE I. Grid Current Before and After Compensation

| Order | Before compensation | | After compensation | |
|---|---|---|---|---|
| | Phase A | Phase B | Phase A | Phase B |
| 1st (Active) | 5 A | 0 A | 3.95 A | 4.15 A |
| 1st (Reactive) | 2 A | 2 A | 1.84 A | 1.3 A |
| 3rd | 0 A | 0 A | 0.06 A | 0.16 A |
| 5th | 2 A | 0 A | 0.06 A | 0.04 A |
| 7th | 1.6 A | 0 A | 0.03 A | 0.02 A |
| 9th | 0 A | 1 A | 0.01 A | 0.01 A |
| 11th | 0.8 A | 0 A | 0.01 A | 0.01 A |
| 13th | 0.4 A | 0.4 A | 0.02 A | 0.02 A |

The simulation process is organized as below.

As shown in Fig. 9, the harmonic compensation is enabled at 0.25 s. From Table I it reduces the total harmonic distortion (THD) of the Phase A current from 23.4% to 5.8% and the Phase B current reduces from 19.8% to 5.9%.

At 0.45 s, the power balancing function is activated. The power is averaged over the two phases. Before imbalance compensation, the current is 5.4 A on Phase A and 2 A on Phase B. After phase imbalance compensation, the current is 6 A on each phase. The results are shown in Fig. 10.

At 0.6 s, the RPR starts to compensate the reactive power to the utility grid. The grid reactive current reduces from 2 A to 1.84 A and from 2 A to 1.3 A on the two phases respectively. The results are shown in Fig. 11. The simulation waveform is as shown in Figs. 8-11 and Table I. The simulation results show that the RPR can compensate the reactive power, current harmonics, and balance the power of the two phases. Therefore. the PQRR controller can provide good compensation for the current harmonics components.

### B. Experiment Studies

A 2 kW experimental prototype, which is shown in Fig. 12 and Fig. 13, was built to verify the RPR proposed in this paper. The low voltage dc side is connected to a 2 kW PV boost converter and a 500 W bidirectional dc/dc converter. The ac side of the RPR is connected to an 110V/110V split-phase grid. It should be noted that a three-winding transformer is applied to generate the split-phase voltage. The LCL filter design for the inverter can be found in [21].

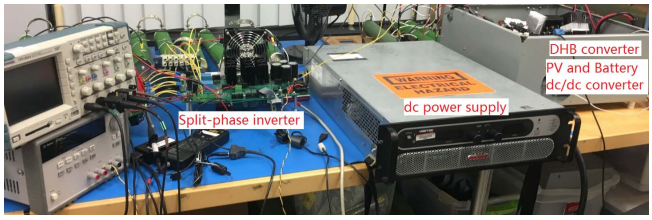


Fig. 12. Experimental prototype of the RPR.

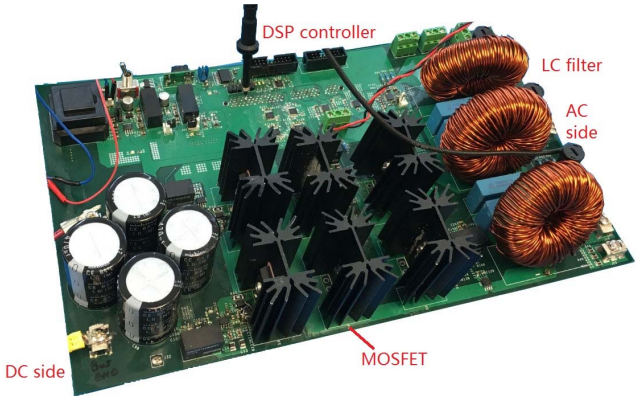


Fig. 13. Split-phase inverter.

The first group of experiments is in islanded mode. Fig. 14 and Fig. 15 show the experimental results for the balanced load for islanded mode. The load is a 1.3 kW power resistor bank between the two phases. Fig. 14 shows the output waveform of the split-phase inverter.

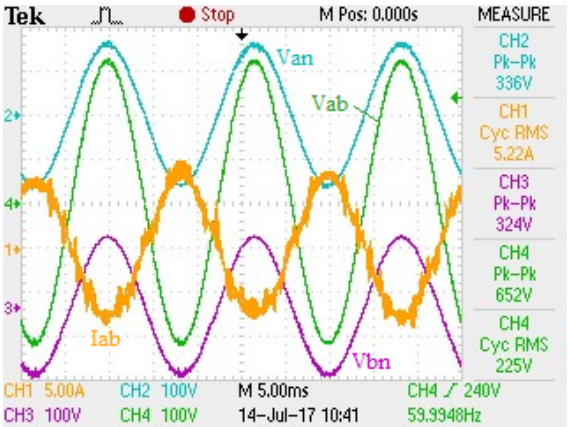


Fig. 14. The waveform of the split-phase inverter.(CH1: Phase A current; CH2: Phase A voltage; CH3: Phase B voltage; CH4: Line-to-line voltage)

Fig. 15 is the waveform from the dc side of the RPR. From Fig. 15, it is shown that the DHB converter works under ZVS mode. From Fig. 14 and Fig. 15, the proposed RPR and its control strategy can satisfy the power quality requirements for the residential load. Using MATLAB to analyze the waveforms, the THD of the voltage is 1.4%. It should be noted that the higher-order harmonics of the current, such as CH1 (yellow) of Fig. 14, CH1(yellow) and CH4(green) of Fig. 15, come from the measurement. When the current probe is closed to the filter inductor, the flux of the inductor may generate EMI noise on the oscilloscope channel.

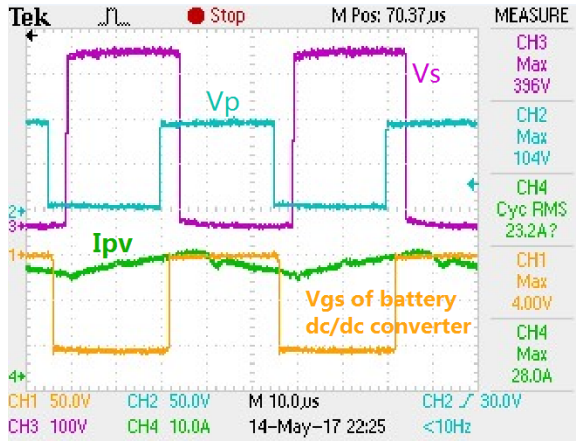


Fig. 15. The waveform of the DHB converter and PV boost converter. .(CH1: Vgs signal of battery dc/dc converter; CH2: Primary side voltage of DHB; CH3: Secondary side voltage of DHB; CH4: Inductor current of the PV boost converter)

The second group of experiments is islanded mode. In this group the load is imbalanced. There is a 500 W load on Phase A and a 0 W load on Phase B. From Fig. 16, the experimental result, the split-phase inverter can provide power to the imbalanced load. It should be noted that, for the light-load condition, the effect of the filter is not as good as the heavy-load phase. Thus, the Phase B voltage is a little distorted. Better control parameters can alleviate this problem.

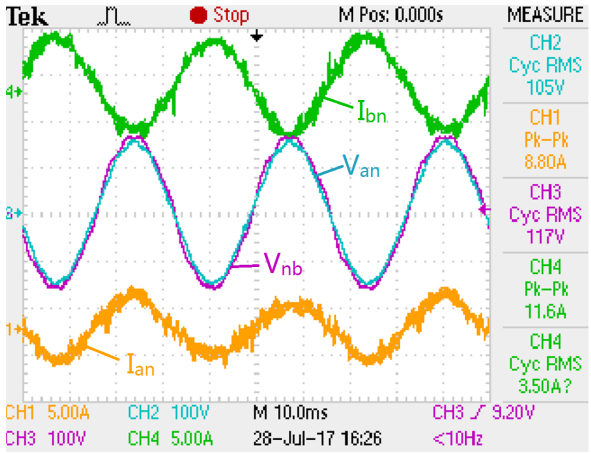


Fig. 16. The waveform of the split-phase inverter for islanding mode. (CH1: Phase A current; CH2: Phase A voltage; CH3: Phase B voltage(inverted); CH4:Phase B current)

The third group is the grid-connected mode. In this group the load is imbalanced. There is a 400 W load on Phase A and a 80 W load on Phase B. Fig. 17 is the experimental result after phase imbalance compensation is activated. The imbalanced load is compensated by the split-phase inverter.

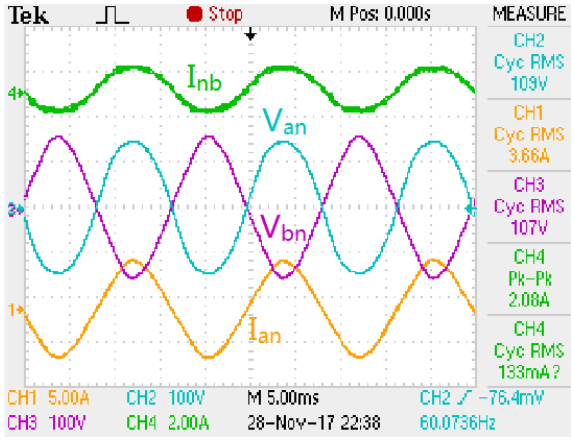


Fig. 17. The waveform of the split-phase inverter for islanding mode. (CH1: Phase A current; CH2: Phase A voltage; CH3: Phase B voltage; CH4:Phase B current(inverted))

From the experiment results, the proposed RPR and its control strategy can deliver the power from the PV terminal and batteries to the community grid. When the load is not balanced on the two phases, the RPR can adjust the power distribution on the two phases.

## VI. CONCLUSIONS

In this paper, a RPR for addressing the power quality issues for the distribution grid is proposed. It serves not only to manage the storage system and DGs in the home, but also to compensate the harmonics, reactive power and imbalanced power. A PQRR controller is adopted for the proposed RPR. The simulation and experimental results show the functionality of the proposed RPR.


## ACKNOWLEDGMENT

Special appreciation goes to the National Science Foundation Industry/University Cooperative Research Center on GRid-connected Advanced Power Electronic Systems (GRAPES) members, the sponsors of this project.


## REFERENCES


[1] D. E. Olivares, A. Mehrizi-Sani, et al., "Trends in microgrid control," *IEEE Transactions on Smart Grid*, vol. 5, no. 4, pp. 1905–1919, 2014.

[2] P. H. Nguyen, W. L. Kling and P. F. Ribeiro, "Smart Power Router: A Flexible Agent-Based Converter Interface in Active Distribution Networks," *IEEE Transactions on Smart Grid*, vol. 2, no. 3, pp. 487-495, Sept. 2011.

[3] M. R. Elhebeary, M. A. A. Ibrahim, M. M. Aboudina and et al,, "Dual-Source Self-Start High-Efficiency Microscale Smart Energy Harvesting System for IoT," I*EEE Transactions on Industrial Electronics*, vol. 65, no. 1, pp. 342-351, Jan. 2018.

[4] R. Gao, X. She, I. Husain and A. Q. Huang, "Solid-State-Transformer-Interfaced Permanent Magnet Wind Turbine Distributed Generation System With Power Management Functions," *IEEE Transactions on Industry Applications*, vol. 53, no. 4, pp. 3849-3861, Jul-Aug 2017.

[5] S. Kouro, et al., "Recent Advances and Industrial Applications of Multilevel Converters," *IEEE Transactions on Industrial Electronics*, vol. 57, no. 8, pp. 2553-2580, Aug. 2010.

[6] S. Han and J. Lee, "An overview of peak-to-average power ratio reduction techniques for multicarrier transmission," *IEEE Wireless Communications*, vol. 12, no. 2, pp. 56-65, Apr 2005.

[7] M. Liserre, F. Blaabjerg and S. Hansen, "Design and control of an LCL-filter-based three-phase active rectifier," *IEEE Transactions on Industry Applications*, vol. 41, no. 5, pp. 1281-1291, Sept.-Oct. 2005.

[8] D. Hogan, F. Gonzalezl, et al., "An Adaptive Digital Control Scheme for Improved Active Power Filtering under Distorted Grid Conditions," *IEEE Transactions on Industrial Electronics*, vol. PP, no. 99, pp. 1-1.

[9] Y. Li and J. He, "Distribution System Harmonic Compensation Methods: An Overview of DG-Interfacing Inverters," *IEEE Industrial Electronics Magazine*, vol. 8, no. 4, pp. 18-31, Dec. 2014.

[10] V. Jones and J. C. Balda, "Correcting current imbalances in three-phase four-wire distribution systems," in *Proc. of 2016 IEEE Applied Power Electronics Conference and Exposition* (*APEC*), Long Beach, CA, 2016, pp. 1387-1391.

[11] R. H. Salim and R. A. Ramos, "A framework for analyzing the small-signal dynamic performance of unbalanced power systems," in *Proc. of IEEE 2011 Power and Energy Society General Meeting*, San Diego, CA, 2011, pp. 1-8.

[12] S. Inoue, T. Shimizu and K. Wada, "Control Methods and Compensation Characteristics of a Series Active Filter for a Neutral Conductor," *IEEE Transactions on Industrial Electronics*, Vol. 54, No. 1, pp. 433-440, Feb. 2007.

[13] Y. Kuo, T. Liang and J. Chen, "A high-efficiency single-phase three-wire photovoltaic energy conversion system," *IEEE Transactions on Industrial Electronics*, vol. 50, no. 1, pp. 116-122, Feb 2003.

[14] S. Zhao, Y. Zhang, J. Moquin and H. A. Mantooth, "The hierarchical energy management control for residential energy harvesting system," in *Proc. of IEEE Energy Conversion Congress and Exposition (ECCE)*, Milwaukee, WI, 2016, pp. 1-7.

[15] D. Li and Z. Q. Zhu, "A Novel Integrated Power Quality Controller for Microgrid," *IEEE Transactions on Industrial Electronics*, vol. 62, no. 5, pp. 2848-2858, May 2015.

[16] X. Sun et al., "Study of a Novel Equivalent Model and a Long-Feeder Simulator-Based Active Power Filter in a Closed-Loop Distribution Feeder," *IEEE Transactions on Industrial Electronics*, vol. 63, no. 5, pp. 2702-2712, May 2016.

[17] S. Zhao, J. Umuhoza, Y. Zhang, J. Moquin, C. Farnell and H. A. Mantooth, "Analysis and optimization of a high-efficiency residential energy harvesting system with dual half-bridge converter," in *Proc. of 2017 IEEE Applied Power Electronics Conference and Exposition (APEC)*, Tampa, FL, 2017, pp. 2838-2844.

[18] Ó. Lucía, I. Cvetkovic, et al., "Design of Home Appliances for a DC-Based Nanogrid System: An Induction Range Study Case," *IEEE Journal of Emerging and Selected Topics in Power Electronics*, vol. 1, no. 4, pp. 315-326, Dec. 2013.

[19] F. Liu, Y. Zhou, and et al., "Parameter Design of a Two-Current-Loop Controller Used in a Grid-Connected Inverter System With LCL Filter," *IEEE Transactions on Industrial Electronics*, vol. 56, no. 11, pp. 4483-4491, Nov. 2009.

[20] D. Chen, L. Xu and L. Yao, "DC Voltage Variation Based Autonomous Control of DC Microgrids," *IEEE Transactions on Power Delivery*, vol. 28, no. 2, pp. 637-648, April 2013.

[21] Y. Liu, A. H. Mantooth, J. C. Balda and C. Farmell, "A Variable Inductor Based LCL Filter for Large-Scale Microgrid Application," *IEEE Transactions on Power Electronics*, vol. PP, no. 99, pp. 1-1.